

## Supplementary Materials for

### Scalable solution-phase epitaxial growth of symmetry-mismatched heterostructures on two-dimensional crystal soft template

Zhaoyang Lin, Anxiang Yin, Jun Mao, Yi Xia, Nicholas Kempf, Qiyuan He, Yiliu Wang, Chih-Yen Chen, Yanliang Zhang, Vidvuds Ozolins, Zhifeng Ren, Yu Huang, Xiangfeng Duan

Published 7 October 2016, *Sci. Adv.* **2**, e1600993 (2016)  
DOI: 10.1126/sciadv.1600993

#### This PDF file includes:

- fig. S1. PXRD pattern for the PbSe/Bi<sub>2</sub>Se<sub>3</sub> heterostructure.
- fig. S2. HRTEM analysis of the pure Bi<sub>2</sub>Se<sub>3</sub> region in the PbSe/Bi<sub>2</sub>Se<sub>3</sub> heterostructure.
- fig. S3. Low-magnification representative STEM image of the PbSe/Bi<sub>2</sub>Se<sub>3</sub> heterostructure.
- fig. S4. High-magnification representative STEM image of the PbSe/Bi<sub>2</sub>Se<sub>3</sub> heterostructure.
- fig. S5. Atomic crystal structure for the intrinsic and expanded Bi<sub>2</sub>Se<sub>3</sub> (0001) layers.
- note S1. DFT modeling of PbSe (001)–Bi<sub>2</sub>Se<sub>3</sub> (001), PbSe (011)–Bi<sub>2</sub>Se<sub>3</sub> (0001), and PbSe (111)–Bi<sub>2</sub>Se<sub>3</sub> (0001) interfaces.

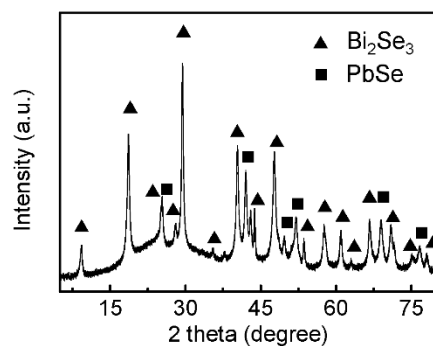


**fig. S1. PXRD pattern for the PbSe/Bi<sub>2</sub>Se<sub>3</sub> heterostructure.**

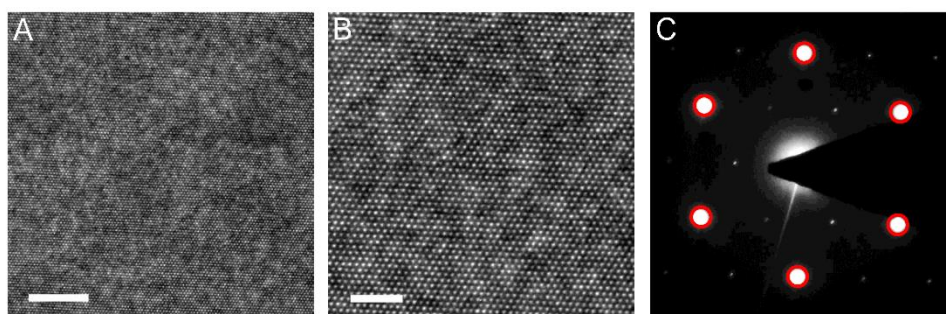


**fig. S2. HRTEM analysis of the pure Bi<sub>2</sub>Se<sub>3</sub> region in the PbSe/Bi<sub>2</sub>Se<sub>3</sub> heterostructure. (A, B)**

HRTEM image of the pure Bi<sub>2</sub>Se<sub>3</sub> region in the PbSe/Bi<sub>2</sub>Se<sub>3</sub> heterostructure as shown in Fig. 2A. Scale bars are 5 nm and 2 nm in (A) and (B). (C) SAED taken from the area in (B) with the guiding label to feature the symmetry of the diffraction spots.

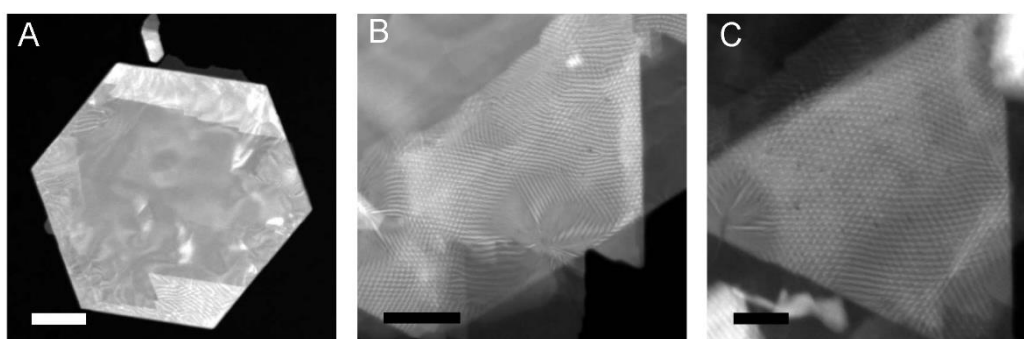


**fig. S3. Low-magnification representative STEM image of the PbSe/Bi<sub>2</sub>Se<sub>3</sub> heterostructure.**

Scale bars, 100 nm (A) and (B), 50 nm for (C).

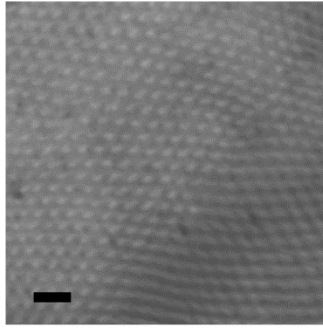


**fig. S4. High-magnification representative STEM image of the PbSe/Bi<sub>2</sub>Se<sub>3</sub> heterostructure.** Scale bar is 20 nm.

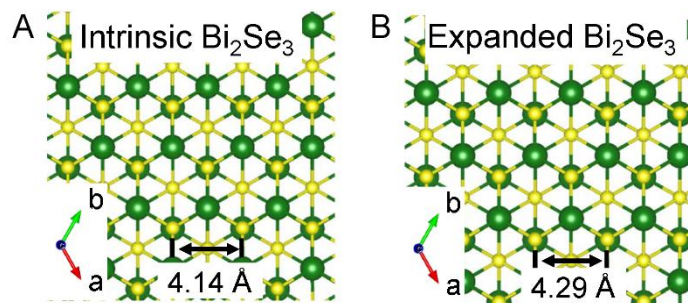


**fig. S5. Atomic crystal structure for the intrinsic and expanded Bi<sub>2</sub>Se<sub>3</sub> (0001) layers.** (A, B) Atomic crystal structure for the intrinsic (A) and expanded (B) Bi<sub>2</sub>Se<sub>3</sub> (0001) layers.

**note S1. DFT modeling of PbSe (001)–Bi<sub>2</sub>Se<sub>3</sub> (001), PbSe (011)–Bi<sub>2</sub>Se<sub>3</sub> (0001), and PbSe (111)–Bi<sub>2</sub>Se<sub>3</sub> (0001) interfaces.**

Our DFT modeling of stability of interface structures mainly consists of two parts, namely constructing interface structure and calculating interfacial energy. In order to theoretically confirm the energetic preference of PbSe (001)–Bi<sub>2</sub>Se<sub>3</sub> (0001) interface, we constructed various 2D periodic interfaces that contain commensurate slabs of Bi<sub>2</sub>Se<sub>3</sub> and PbSe. Since PbSe grows on Bi<sub>2</sub>Se<sub>3</sub> substrate and quintuple layers in Bi<sub>2</sub>Se<sub>3</sub> are separated by van der Waals gap, we choose single quintuple layer of Bi<sub>2</sub>Se<sub>3</sub> as the substrate. Three typical surfaces of PbSe, namely (001), (011) and (111) were then connected with the single quintuple layer to form interfaces. In constructing the 2D periodic interfaces we expand the lattice

parameter (4.185 Å) of fully relaxed single quintuple layer of Bi<sub>2</sub>Se<sub>3</sub> to be the nearest Pb-Pb distance of 4.389 Å. PbSe (001) and PbSe (011) slabs were slightly expanded by 1% and 2% along [110] and [001] directions respectively in the corresponding supercell interface structures to satisfy the commensurate requirement. The orientation inside the interface was determined by setting the bonds between Pb from PbSe slab and Se from Bi<sub>2</sub>Se<sub>3</sub> slab in the z-direction and the distance between PbSe and Bi<sub>2</sub>Se<sub>3</sub> slabs was further assumed as the Pb-Se bond length (3.103 Å) in PbSe bulk phase. The 2D PbSe (111)-Bi<sub>2</sub>Se<sub>3</sub> (0001) interface structure has the same periodicity as that of single quintuple layer and each unit has 2 Pb, 2 Bi and 5 Se atoms. Both 2D PbSe (100)-Bi<sub>2</sub>Se<sub>3</sub> (0001) and PbSe (011)-Bi<sub>2</sub>Se<sub>3</sub> (0001) interface structures have an orthorhombic unit cell with lattice parameter of a (a=4.389 Å) and  $4\sqrt{3}a$  along the interface axis. And each unit cell contains 21 Pb, 16 Bi, 45 Se and 15 Pb, 16 Bi, 39 Se atoms respectively. Then we fully relaxed these structures and calculated the total energies. To compare the relative stability of various interfaces, we estimate the interfacial energy without considering the entropic and volumetric contributions. All interface structures are further assumed in chemical and thermal equilibria with bulk phases. The formation energy per area, defined as the interfacial energy, can be expressed as

$$\Delta E_{\text{Bi}_2\text{Se}_3-\text{PbSe}} = \frac{1}{2S_{\text{Bi}_2\text{Se}_3-\text{PbSe}}} \left( E_{\text{Bi}_2\text{Se}_3-\text{PbSe}}^i - xE_{\text{Bi}_2\text{Se}_3}^b - yE_{\text{PbSe}}^b \right)$$

where  $S_{\text{Bi}_2\text{Se}_3-\text{PbSe}}$  is the area of the interface,  $E_{\text{Bi}_2\text{Se}_3-\text{PbSe}}^i$ ,  $E_{\text{Bi}_2\text{Se}_3}^b$  and  $E_{\text{PbSe}}^b$  are the energies of interface structure, bulk phases of Bi<sub>2</sub>Se<sub>3</sub> and PbSe. The x and y represent the numbers of formula unit of bulk phases contained in the interface structure.

The fully relaxed interface structures are shown in Fig. 4. We find that the interface bonds between Pb and Se are all elongated after full relaxation, which means additional bonds along the growing axis are

not preferred. This might be due to the coordination nature of outmost-layer Se in the single quintuple layer of  $\text{Bi}_2\text{Se}_3$ . For the  $\text{PbSe}$  (111)- $\text{Bi}_2\text{Se}_3$  (001) interface the Pb-Se bond increases from 3.103 Å to 3.588 Å. This dramatic change indicates the instability, which is further confirmed by the formed layered structure of  $\text{PbSe}$  slabs. The calculated interfacial energies are shown in Fig. 4. Our result shows that the  $\text{PbSe}$  (001)- $\text{Bi}_2\text{Se}_3$  (001) interface has the lowest interfacial energy, which naturally confirms the experimental measurements. This is mainly due to the larger interfacial energy needed to cleave the bulk phase of  $\text{PbSe}$  either through the (011) or (111) planes. This would directly give rise to higher formation energy since there is no obvious bonds found between Pb and Se in the interface region.